International Journal of Advanced Engineering Research and Science (IJAERS)
Peer-Reviewed Journal
ISSN: 2349-6495(P) | 2456-1908(O)
Vol-12, Issue-5; May, 2025
Journal Home Page Available: https://ijaers.com/
Article DOI: https://dx.doi.org/10.22161/ijaers.125.6

Diffraction Model on the Breakwater Gap Based on Velocity Potential Equation

Syawaluddin Hutahaean

Ocean Engineering Program, Faculty of Civil and Environmental Engineering-Bandung Institute of Technology (ITB), Bandung 40132, Indonesia.
syawalf1@yahoo.co.id

Received: 19 Apr 2025,

Receive in revised form: 17 May 2025,

Accepted: 21 May 2025,

Available online: 25 May 2025

Keywords*— *diffraction, break water gap, velocity potential equation

***Abstract*—** *In this research, the governing equation for wave diffraction at a breakwater gap is formulated. The equation is derived by substituting the three-dimensional velocity potential—obtained as the solution to the Laplace equation—into the Laplace equation, under the condition that there is a variation or differential in the wave constants. The resulting equation is a second-order partial differential equation with respect to one of the wave constants. The governing equation is then solved numerically using the Finite Difference Method, employing the Successive Over Relaxation (SOR) technique for the iterative calculation.*

I. INTRODUCTION

Considering the needs of proper ports and the limited availability of naturally sheltered waters, there is an increasing trend toward the construction of enclosed ports, which are protected by breakwaters. The primary function of the breakwater in this context is to attenuate waves from the open sea, thereby creating a calm, sheltered area on the leeward side. This reduction in wave activity is essential to facilitate safe and efficient loading and unloading operations for vessels. An illustration of an enclosed port protected by breakwaters is presented in Figure (1).

Waves from the open sea can enter the sheltered area through the breakwater opening or entrance. The wave conditions within the lee side are primarily influenced by the width of this entrance. However, the entrance width is mainly determined by navigational safety and the operational needs of ship traffic, meaning that reducing the wave height on the lee side cannot simply be achieved by narrowing the entrance. The berthing zone is a critical area that must be ensured safe and calm. In cases where navigational requirements necessitate a wide entrance, leading to significant wave penetration into the berthing area, the distance between the entrance and the berthing zone is typically extended to create a calmer environment for vessel operations.

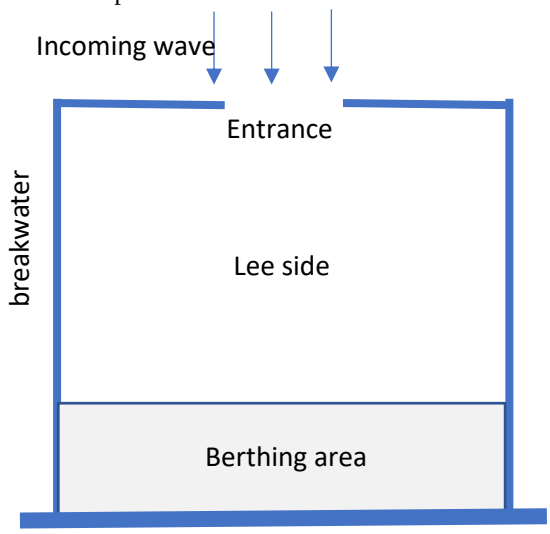

Fig.1: Enclosed Port

To analyze the wave conditions within the lee side, wave diffraction models are commonly applied to simulate wave behavior at the breakwater opening. These models have been extensively developed, generally utilizing time series models.

In the present research, a wave diffraction model is developed based on the velocity potential equation, which is a solution to the Laplace equation. The adoption of a velocity potential-based approach aims to develop a model that is both simpler and more practical to apply in engineering analyses.

II. THE GOVERNING EQUATION

The velocity potential for a wave propagating along the horizontal axis ξ, is given as the solution to the Laplace equation, as presented by Dean (1991):

$$\phi(\xi,z,t) = G(\cos k\xi + \sin k\xi)\cosh k(h+z)\sin\sigma t \quad \dots(1)$$

Where $k = \frac{2\pi}{L}$ is the wave number, L is the wavelength , $\sigma = \frac{2\pi}{T}$, T is the wave period and G is the wave constant.

The horizontal axis ξ is inclined at an angle α relative to the x on (x,y), Fig (2). The velocity potential of the wave in the (x,y,z) as proposed by Dean (1991) is,

$$\phi(x,y,z,t) = G(\cos k(x\cos\alpha) + \sin k(y\sin\alpha))\cosh k(h+z)\sin\sigma t \quad \dots(2)$$

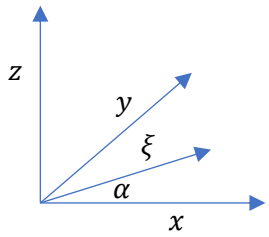

Fig.2: Axis system.

Laplace's equation for the three-dimensional Cartesian coordinate system (x,y,z) is,

$$\frac{\partial^2\phi}{\partial x^2} + \frac{\partial^2\phi}{\partial y^2} + \frac{\partial^2\phi}{\partial z^2} = 0 \quad \dots(3)$$

The substitution of (2) to (3) by introducing the differentials G and k, a set of differential equations for G and k is formed. This derivation is further simplified by considering the characteristic point where

$$\cos k(x\cos\alpha) + \sin k(y\sin\alpha) = \sin k(x\cos\alpha) + \cos k(y\sin\alpha)$$

The conservation equation for G is,

$$\frac{\partial^2 G}{\partial x^2} + \frac{\partial^2 G}{\partial y^2} = 0 \quad \dots(4)$$

This equation is used as the governing equation for modeling diffraction at a breakwater gap. In this research, diffraction is defined as the spreading or transfer of wave energy in the lateral direction. Accordingly, in Equation (4), the wave direction is along the x-axis, while energy transfer occurs along the y-axis.

Equation (4) serves as the governing equation for modeling wave diffraction through the breakwater gap. Notably, this equation does not incorporate the water depth variable, limiting its applicability to scenarios with uniform water depth. Nevertheless, even under constant depth conditions, variations in G may still occur due to diffraction processes, which redistribute wave energy and subsequently alter the wave amplitude. Although Equation (4) was formulated under the assumption that k may vary spatially, no differentials of k appear in the equation itself. Therefore, in practical applications, k is treated as a constant, typically corresponding to its value at the entrance of the breakwater. Hutahaean (2023) proposed a wave amplitude function describing the relationship between the wave amplitude A and G, k and σ. This formulation was later refined by Hutahaean (2025), who introduced an updated weighting coefficient within the truncated Taylor series expansion, yielding:

$$A = \frac{2Gk}{\gamma_{t,2}\sigma}\cosh\theta\pi\left(\tanh\theta\pi - \frac{\gamma_{x,2}kA}{2}\right) \quad \dots(5)$$

Hutahaean (2025), also obtained another form of wave amplitude function as follows

$$A = \frac{\sqrt{2}\,Gk}{\gamma_{t,2}\sigma}\sinh\theta\pi \quad \dots(6)$$

In Equations (5) and (6), $\gamma_{t,2}$ and $\gamma_{x,2}$ represent weighting coefficient. In the present research, these coefficients are taken as $\gamma_{t,2} = 1.999773$, $\gamma_{x,2} = 0.999733$. The detailed formulation of these weighting coefficients can be found in Hutahaean (2025). The parameter θ in both equations denotes the deep water coefficient, for which $\tanh\theta\pi \approx 1.0$ in this research is $\theta = 3$. With identical inputs, both Equations (5) and (6) yield the same wave amplitude.

Once the value of G on the lee side from (4) is obtained, the wave amplitude A and wave height H, could be measured based on the wave number k at the entrance.

Solving Equation (4) requires the specification of the G value at the entrance. When the entrance is situated in deep water, the wave constants can be calculated using the following equations:

$$k_0 = \frac{\tanh\theta\pi}{\gamma_{x,2}A_0}\left(2-\sqrt{2}\right) \quad \dots(7)$$

$$\sigma^2 = \frac{gk_0\tanh\theta\pi}{\sqrt{2}\gamma_{t,2}\gamma_{t,3}} \quad \dots.(8)$$

$\gamma_{t,3} = 3.049333$ is the weighting coefficient, A_0 is the known wave amplitude at deep water depth. The derivation

of these equations is presented in Hutahaean (2025). The condition for deep water depth is given by,

$$h_0 \geq \frac{\theta\pi}{k_0} - \frac{A_0}{2} \quad \ldots (9)$$

Both Equations (5) and (6) can be rearranged to express G as a function of the wave amplitude A as follows:

$$G_0 = \frac{\gamma_{t,2}\sigma A_0}{2\, k_0 \cosh\, \theta\pi \left(\tanh\theta\pi - \frac{\gamma_{x,2} k_0 A_0}{2}\right)} \quad \ldots (10)$$

$$G_0 = \frac{\gamma_{t,2}\sigma A_0}{\sqrt{2}\, k_0 \sinh\, \theta\pi} \quad \ldots . (11)$$

Using these equations, the value of G_0 at the entrance can be calculated. Table (1) presents the computed values of k_0, σ, G_0 and h_0 for several wave amplitudes A_0, where the wave height $H_0 = 2\, A_0$. In scenarios where the entrance is located at a water depth h $h < h_0$, a wave transformation analysis is required to adjust for the depth transition from $h_0$to h.

Table 1: Wave constant at deep water.

H_0 (m)	k_0 (m^{-1})	σ (sec^{-1})	h_0 (m)	G_0 (m.m/sec)
1	1.173	1.146	7.786	0.00011
1.2	0.977	1.046	9.343	0.00015
1.4	0.838	0.969	10.9	0.00018
1.6	0.733	0.906	12.458	0.00023
1.8	0.652	0.854	14.015	0.00027
2	0.586	0.81	15.572	0.00032
2.2	0.533	0.773	17.129	0.00036
2.4	0.489	0.74	18.686	0.00041
2.6	0.451	0.711	20.244	0.00047
2.8	0.419	0.685	21.801	0.00052

III. NUMERICAL SOLUTION

Equation (4) is classified as an elliptic partial differential equation, which represents a boundary value problem requiring appropriate boundary conditions for its solution. The boundary conditions applied in this research are as follows:,

a. A Dirichlet boundary condition is applied at the breakwater entrance, where the value of $G = c$, where c is a known constant.

b. A Neuman boundary condition, representing a solid boundary, is applied along the breakwater walls on the lee side, expressed as: $\frac{\partial G}{\partial n} = 0$, where n is the axis normal to the breakwater wall. Along the wall parallel to the axis y, $\frac{\partial G}{\partial n} = \frac{\partial G}{\partial x} = 0$ while long the wall parallel to the axis-x, $\frac{\partial G}{\partial n} = \frac{\partial G}{\partial y} = 0$.

The locations where these boundary conditions are applied are illustrated in Fig. (3).

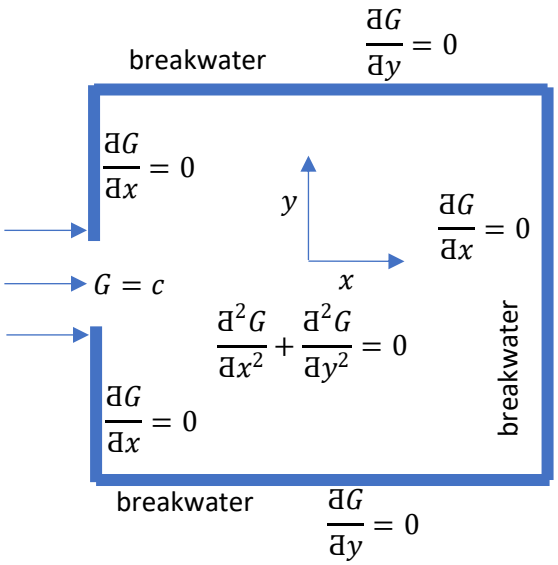

Fig.3: Breakwater sketch and the boundary conditions.

3.1. Finite Difference Method.

Equation (4) is solved using the Finite Difference Method (FDM), in which the computational domain is discretized into a finite number of grid points (Fig. (4)). The governing equation is applied and solved at each grid point within the domain, except at the entrance point.

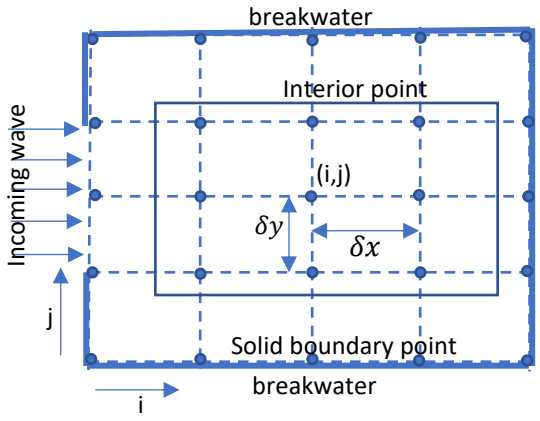

Fig.4: The division of the computational domain into a grid of discrete points.

The finite difference equations are formulated and applied at each grid point within the domain, based on the approach described by Arden, Bruce W., and Astill, Kenneth N. (1970):

a. At interior points within the domain, the central difference scheme is employed

$$\frac{\partial^2 G}{\partial x^2} = \frac{G_{i+1,j} - 2G_{i,j} + G_{i-1,j}}{\delta x^2}$$

$$\frac{\partial^2 G}{\partial y^2} = \frac{G_{i,j+1} - 2G_{i,j} + G_{i,j+1}}{\delta y^2}$$

Substituting these expressions into Equation (4)

$$\frac{G_{i+1,j} - 2G_{i,j} + G_{i-1,j}}{\delta x^2} + \frac{G_{i,j+1} - 2G_{i,j} + G_{i,j+1}}{\delta y^2} = 0$$

This can be rearranged into the standard finite difference equation:

$$2\left(1 + \frac{\delta x^2}{\delta y^2}\right) G_{i,j} = G_{i+1,j} + G_{i-1,j} + \frac{\delta x^2}{\delta y^2}\left(G_{i,j+1} + G_{i,j-1}\right) \dots (9)$$

b. At the solid boundary point

b.1. At the left breakwater (Neuman boundary), a forward difference scheme is used:

$$\frac{\partial G}{\partial x} = \frac{G_{i+1,j} - G_{i,j}}{\delta x} = 0$$

Thus,

$$G_{i,j} = G_{i+1,j} \quad \dots..(10)$$

b.2 At the right breakwater, a backward difference scheme is applied:

$$\frac{\partial G}{\partial x} = \frac{G_{i,j} - G_{i-1,j}}{\delta x} = 0$$

$$G_{i,j} = G_{i-1,j} \quad \dots..(11)$$

b.3. At the lower breakwater, a backward difference scheme is applied:

$$\frac{\partial G}{\partial y} = \frac{G_{i,j+1} - G_{i,j}}{\delta y} = 0$$

$$G_{i,j} = G_{i,j+1} \quad \dots..(12)$$

b.4. At the upper breakwater, a backward difference scheme is applied:

$$\frac{\partial G}{\partial y} = \frac{G_{i,j} - G_{i,j-1}}{\delta x} = 0$$

$$G_{i,j} = G_{i,j-j} \quad \dots..(13)$$

The grid points involved (i,j), $(i+1,j)$, $(i-1,j)$, $(i,j+1)$ and $(i,j-1)$ are presented in Fig (5).

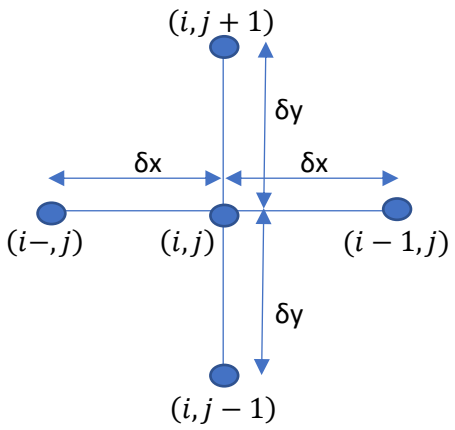

Fig.5: Points on FDM.

3.2. Calculation Method

The numerical solution of Equation (4) is performed iteratively using the Successive Over Relaxation (SOR) method, as described by Chow, C.Y. (1979). The steps of the calculation procedure are as follows:

1. The initial iteration value is defined at all points except the entrance point, where $G_{i,j} = 0$.
2. At the interior point $G_{i,j}$ is calculated using equation (9).
3. At the boundary point, $G_{i,j}$ is calculated using equation (10), (11), (12) and (13).
4. The convergence of all points is checked by verifying that $\left|G_{i,j}^{new} - G_{i,j}^{old}\right| \leq \mu$, where μ is a small positive tolerance, for example $\mu = 0.01$.
5. If any point has not converged, the process returns to Step 2, and the new values of $G_{i,j}$ are recalculated.

Convergence is achieved after a large number of iterations. In this research, with 29,584 points, convergence is attained after 3,000 iterations. Generally, the greater the number of points, the greater the number of iterations required.

The purpose of using this iterative method is to avoid the formation of simultaneous equations or matrices of very large size. This consideration is important since a small grid size is necessary, resulting in a very large number of points, often reaching tens of thousands. For example, for a domain size of 150 m × 150 m, with a grid size of 0.876 m, there are 29,584 points. Without the iterative method, this would require solving a matrix of size 29,584 × 29,584.

3.3. Grid size

The finite difference equations are formulated based on truncating the Taylor series to order 1 or order 2, with the rationale that at sufficiently small grid sizes, the higher-order terms become negligible and can be ignored. Thus, the grid size in the finite difference method (FDM) is chosen such that the higher-order terms in the Taylor series can be safely omitted.

Taylor series for a function x,

$$f(x+\delta x) = f(x) + \delta x \frac{df}{dx} + \frac{\delta x^2}{2}\frac{d^2f}{dx^2} + \frac{\delta x^3}{3!}\frac{d^3f}{dx^3} + \cdots$$

For the Taylor series to be truncated at first order only, the following condition must hold,

$$\left|\frac{\frac{\delta x^2}{2}\frac{d^2f}{dx^2} + \frac{\delta x^3}{3!}\frac{d^3f}{dx^3} + \cdots}{\delta x \frac{df}{dx}}\right| \leq \varepsilon_x \qquad \ldots(14)$$

As a first approximation, it is assumed that δx is very small $\left|\frac{\delta x^3}{3!}\frac{d^3f}{dx^3} + \frac{\delta x^4}{4!}\frac{d^4f}{dx^4} + \cdots\right| \ll \left|\frac{\delta x^2}{2}\frac{d^2f}{dx^2}\right|$. Therefore, equation (14) can be simplified as

$$\left|\frac{\frac{\delta x^2}{2}\frac{d^2f}{dx^2}}{\delta x \frac{df}{dx}}\right| \leq \varepsilon_x$$

Or,

$$\left|\frac{\frac{\delta x}{2}\frac{d^2f}{dx^2}}{\frac{df}{dx}}\right| \leq \varepsilon_x$$

Equation (4) is derived from the Laplace equation, whose solution is a sinusoidal function. Therefore, the function $f(x)$ is taken as a sinusoidal function.

$f(x) = \cos kx$

$$\frac{df}{dx} = -k \sin kx$$

$$\frac{d^2f}{dx^2} = -k^2 \cos kx$$

$$\left|\frac{\frac{\delta x}{2} k \cos kx}{\sin kx}\right| \leq \varepsilon$$

At the characteristic point where $\cos kx = \sin kx$,

$$\frac{\delta x}{2} k \leq \varepsilon_x$$

considering $k = \frac{2\pi}{L}$ and taking the equality sign yields,

$$\delta x = \frac{\varepsilon_x}{\pi} L \qquad \ldots(15)$$

Equation (15) gives a very small grid size. To allow for a larger grid size, the Taylor series expansion is extended up to the fourth order, under the assumption that,

$$\left|\frac{\delta x^5}{5!}\frac{d^5f}{dx^5} + \frac{\delta x^6}{6!}\frac{d^6f}{dx^6} + \cdots\right| \ll \left|\frac{\delta x^2}{2}\frac{d^2f}{dx^2} + \frac{\delta x^3}{3!}\frac{d^3f}{dx^3} + \frac{\delta x^4}{4!}\frac{d^4f}{dx^4}\right|$$

Equation (14) becomes,

$$\left|\frac{\frac{\delta x^2}{2}\frac{d^2f}{dx^2} + \frac{\delta x^3}{3!}\frac{d^3f}{dx^3} + \frac{\delta x^4}{4!}\frac{d^4f}{dx^4}}{\delta x \frac{df}{dx}}\right| \leq \varepsilon_x \qquad \ldots(16)$$

Following similar steps, the equation for δx is obtained as a cubic polynomial,

$$\frac{\delta x}{2}\frac{2\pi}{L} - \frac{\delta x^2}{3!}\left(\frac{2\pi}{L}\right)^2 - \frac{\delta x^3}{4!}\left(\frac{2\pi}{L}\right)^3 - \varepsilon_x = 0 \quad .(17)$$

Table (1) presents the results of the grid size calculations for waves with a wavelength of 16,072 m. It is evident that the grid size obtained from equation (17) is larger than that from equation (15). This indicates that using a longer Taylor series allows for a larger grid size. Since equation (17) is formulated using a fourth-order Taylor series, it provides better accuracy than equation (15).

Table.2: Grid size calculation results

ε_x	δx_{15} (m)	δx_{17} (m)	$\frac{\delta x_{17} - \delta x_{15}}{\delta x_{13}} x100\%$
0.05	0.256	0.265	3.676
0.06	0.307	0.321	4.505
0.07	0.358	0.377	5.373
0.08	0.409	0.435	6.28
0.09	0.46	0.494	7.232
0.1	0.512	0.554	8.232
0.11	0.563	0.615	9.285
0.12	0.614	0.678	10.395
0.13	0.665	0.742	11.571
0.14	0.716	0.808	12.817
0.15	0.767	0.876	14.144

Note : δx_{15}: calculated using equation (15)
δx_{17}: calculated using equation (17)

3.4. Model Results

For example, consider waves with a wave amplitude $A_0 = 1.5\,m$ or $H_0 = 3.0\,m$, a deep water wave constant $k_0 = 0.391$ m^{-1}, $L_0 = 16.072$ m, $T = 9.496$ sec., $\sigma = 0.662$ sec^{-1}, $G_0 = 0.000579$ m.m/sec. For this wave, the deep water depth is $h_0 = 23.358$ m. Diffraction analysis is performed at the breakwater entrance with an entrance width of 40.0 m, approximately 40.0 m≈2.5 L, and a lee side domain of 150 m × 150 m. The water depth is 25 m, which exceeds h_0, classifying the entrance and lee side as deep water;

therefore, no wave transformation analysis from deep water to the entrance is necessary.

Calculations are conducted using a grid size of $\delta x = \delta y = 0.876$ m, obtained based on an accuracy level $\varepsilon_x = 0.15$. The results of the diffraction analysis are presented in Fig. (6).

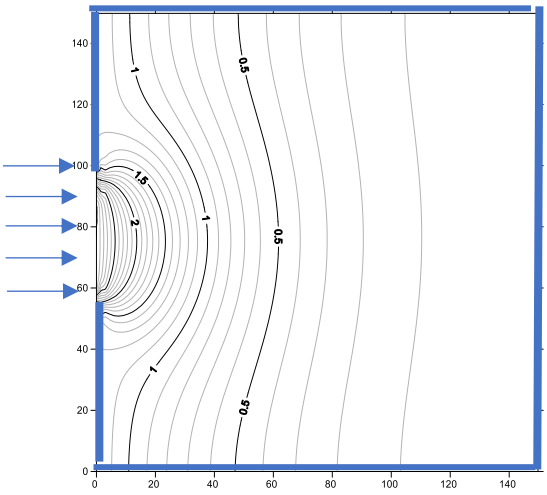

Fig.6: Wave height H contour

In the model results shown in Fig. (6), a very rapid decrease in wave height along the x-axis is observed, starting from an initial wave height $H = 3.0$ m at the entrance, the wave height reduces to 1.0 m at a distance of 30 m. This indicates that the energy transfer in the lateral direction—that is, perpendicular to the wave propagation direction—is excessively large. This behavior contrasts significantly with findings from Penney & Price (1952), Wiegel (1962), and the U.S. Army Coastal Engineering Research Center (1977), where wave height evolution in the wave direction is more gradual.

To align the diffraction results with previous research, equation (4) is modified as follows:

$$\frac{\partial^2 G}{\partial x^2} + \gamma \frac{\partial^2 G}{\partial y^2} 0 \quad \ldots (18)$$

Where γ is a coefficient smaller than 1.0. This coefficient, termed the lateral energy transfer coefficient, quantifies energy transfer in the direction perpendicular to the wave propagation.

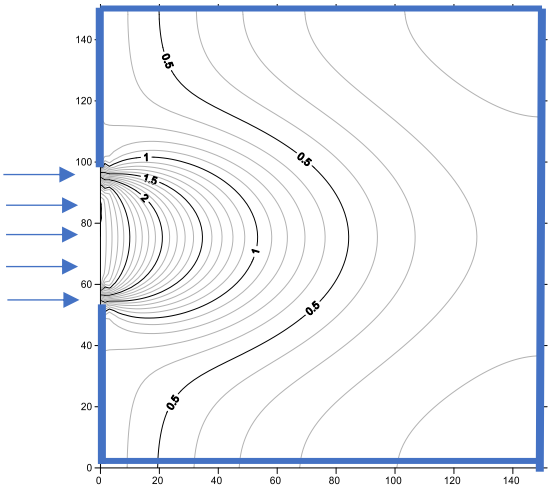

Fig.7: Wave height H contour using $\gamma = 0.25$

Therefore, equation (9) becomes

$$2\left(1 + \gamma \frac{\delta x^2}{\delta y^2}\right) G_{i,j} =$$

$$G_{i+1,j} + G_{i-1,j} + \gamma \frac{\delta x^2}{\delta y^2}\left(G_{i,j+1} + G_{i,j-1}\right) \ldots (19)$$

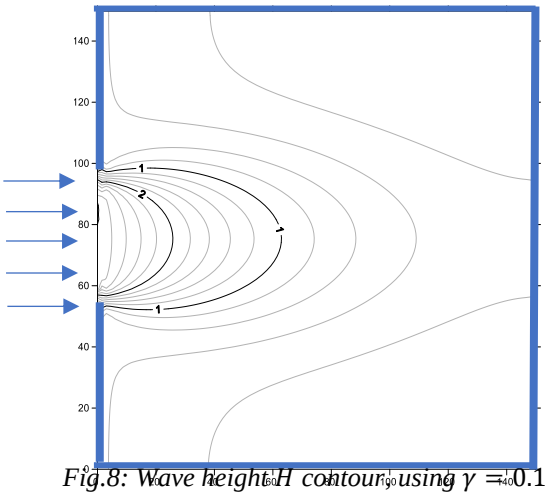

Fig.8: Wave height H contour using $\gamma = 0.125$

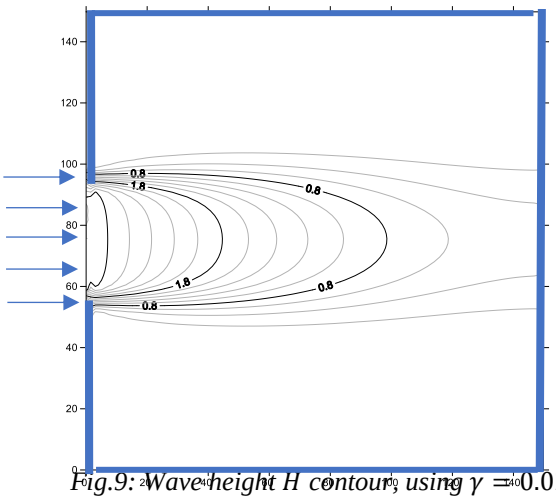

Fig.9: Wave height H contour, using $\gamma = 0.02$

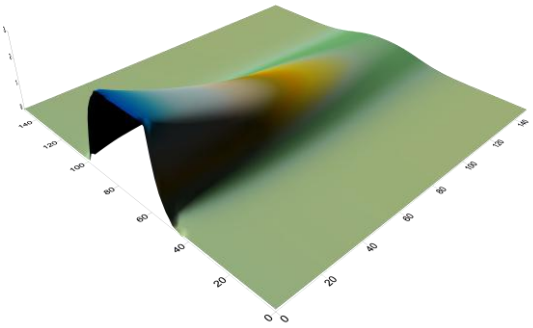

Fig.10: Wave height H contour, 3-D, using $\gamma = 0.02$

Fig. (7) shows the model results for $\gamma = 0.25$, Fig. (8) uses $\gamma = 0.125$, and Fig. (9) uses $\gamma = 0.02$. It is observed that decreasing γ slows the evolution of wave height in the wave direction, indicating a reduction in lateral energy transfer. The calculations using $\gamma = 0.02$ produce results most consistent with previous research findings. The small value of γ thus reflects that lateral energy transfer is minimal.

IV. WAVES FORMING AN ANGLE

In the application of equation (4), the horizontal-x axis must always be aligned with the incoming wave direction. For waves that approach at an angle relative to the breakwater axis, represented by the (ξ, η) coordinate system, the horizontal-x axis will form an angle with the breakwater's horizontal -ξ axis, as shown in Fig. (11). Under these conditions, the grid points generated in the (x, y) coordinate system become non-uniform and irregular.

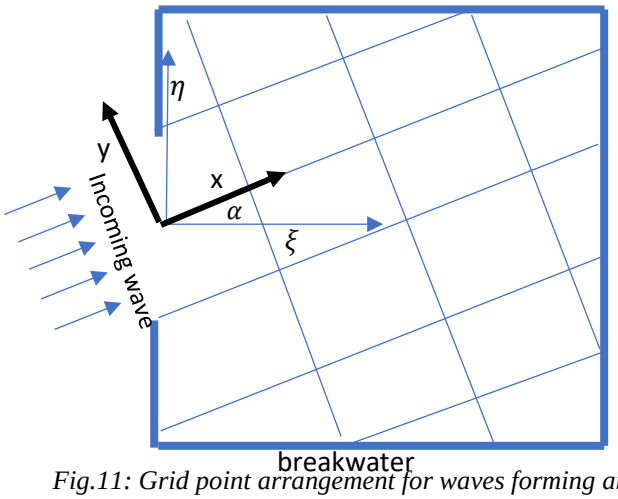

Fig.11: Grid point arrangement for waves forming an angle to the breakwater axis..

In such cases, advanced grid generation methods and numerical techniques that fall outside the scope of the present research are required.

V. CONCLUSION

Overall, the model developed in this research is capable of producing results that align well with previous research findings, indicating that the model can be considered reliable for wave diffraction analysis at breakwater gaps. However, this alignment has been achieved through the adjustment of the lateral energy transfer coefficient. Thus, obtaining reliable values for this coefficient requires further investigation, including laboratory-based physical model studies.

While the governing equation used is relatively simple, involving only a single variable, this simplicity results in an overestimation of lateral energy transfer. If the governing equation were to include the wave number, or the wave number along with the wave direction as variables, it is likely that a more accurate model of lateral energy transfer could be obtained—one that no longer requires an energy transfer coefficient. Consequently, it can be concluded that further research is still needed on the governing equation of the diffraction model.

REFERENCES

[1] Dean, R.G., Dalrymple, R.A. (1991). Water wave mechanics for engineers and scientists. Advance Series on Ocean Engineering.2. Singapore: World Scientific. ISBN 978-981-02-0420-4. OCLC 22907242.

[2] Hutahaean, S. (2023). Water Wave Velocity Potential on Sloping Bottom in Water Wave Transformation Modeling. International Journal of Advance Engineering Research and Science (IJAERS). Vol. 10, Issue 10; Oct, 2023, pp 149-157. Article DOI: https://dx.doi..org/10.22161/ijaers.1010.15.

[3] Hutahaean, S. (2023). New Weighted Taylor Series for Water Wave Energy Loss and Littoral Current Analysis. International Journal of Advance Engineering Research and Science (IJAERS). Vol. 12, Issue 1; Jan, 2025, pp 27-39. Article DOI: https://dx.doi..org/10.22161/ijaers.121.3.

[4] Arden, Bruce W. and Astill Kenneth N. (1970). Numerical Algorithms : Origins and Applcations. Philippines copyright (1970) by Addison-Wesley Publishing Company, Inc.

[5] Penney, W.G., Price, A.T. (1952). The Diffraction Theory of Sea Waves and The Shelter Afforded by Breakwaters. Philos. Trans. Roy. Soc. A, Vol.244 (882), pp. 236-253.

[6] Wiegel, R.L (1962). Diffraction of Waves by a Semi-infinite Breakwater. J. Hydraulics Div., ASCE, Vol.88, No. HYI, pp. 27-44.

[7] U.S. ARMY Coastal Engineering Research Center (1977). Shore Protection Manual, Vol.I, U.S. Government Printing Office, Washington, D.C.